Supplemental Figure 1

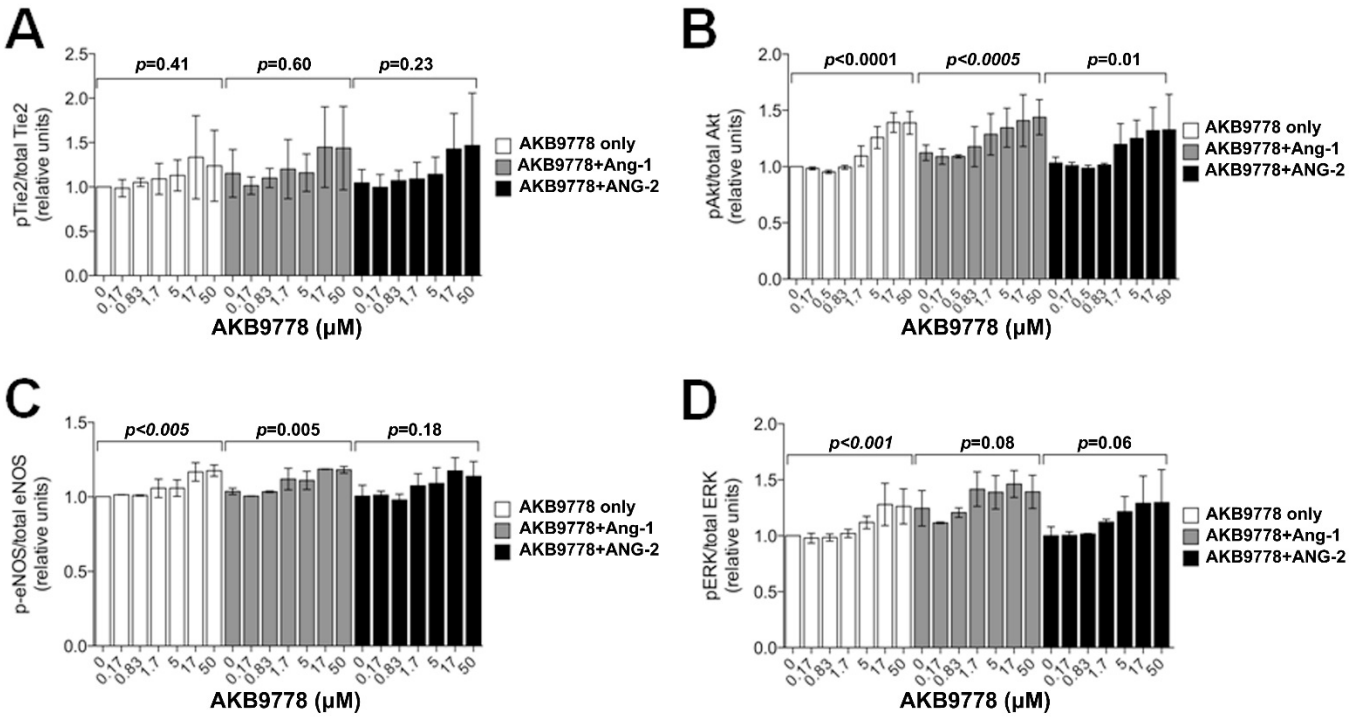

Supplemental Figure 1. Densitometry measurements for immunoblots illustrated in Figure 3.

HUVECs were left untreated or were treated with AKB-9778 alone or together with Ang1 or Ang2, as described in the legend to Figure 2. Experiments were performed 3 to 6 times per condition, and immunoblots were used to quantify protein phosphorylation by densitometry. Bands corresponding to both phosphorylated and total proteins were scanned, and the ratio of phosphorylated to total protein was quantified by densitometry (ImageJ) for phospho-Tie2 (A), phospho-Akt (B), phospho-eNOS (C), and phospho-ERK (D). For each condition, values were normalized to that in the absence of AKB-9778. Differences among groups in each condition were analyzed by one-way ANOVA, and P values are shown for each experiment.

Supplemental Figure 2

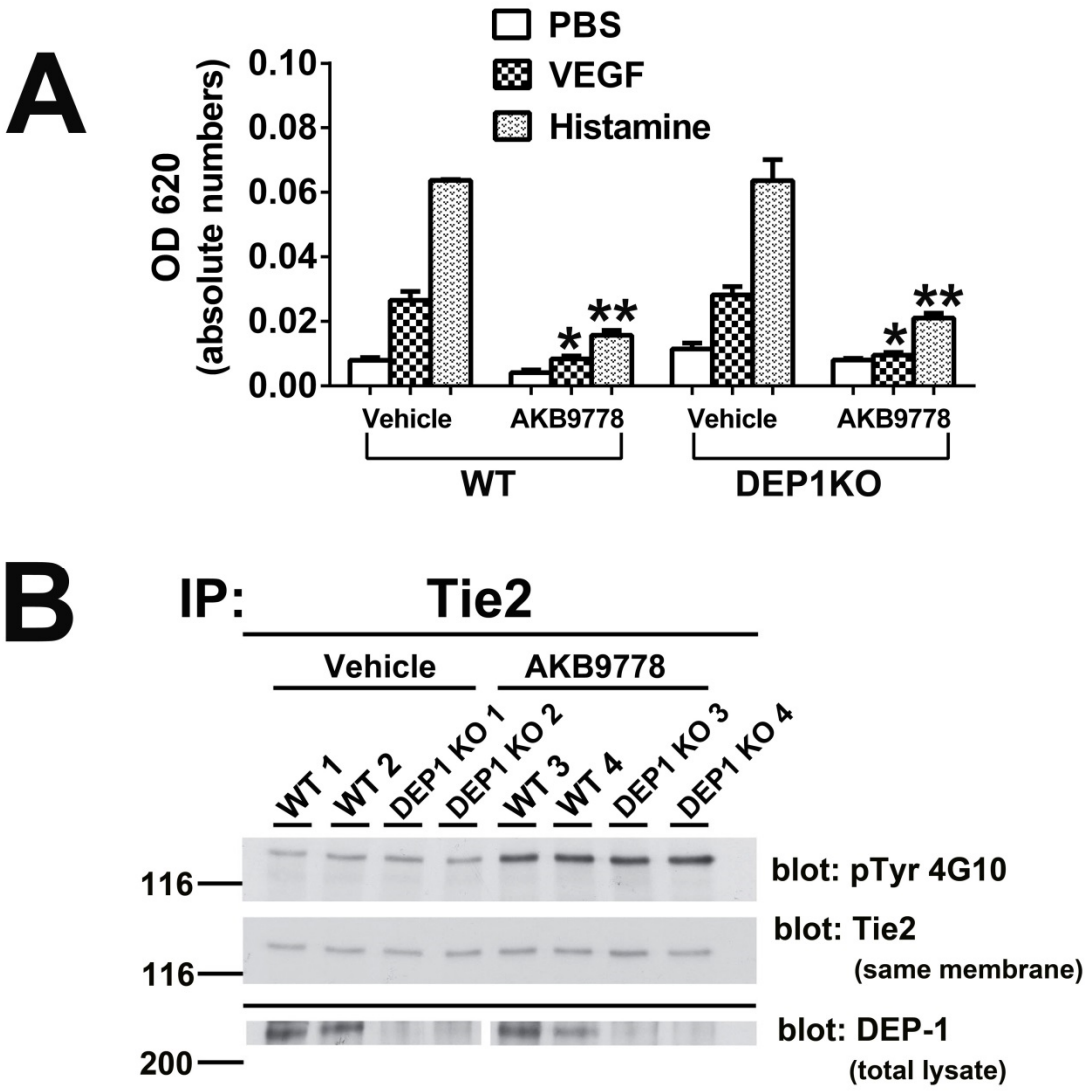

Supplemental Figure 2. Effect of AKB-9778 on VEGF- and histamine-induced leakage in wild type and DEP-1 knockout mice.

(A) Wild type (WT, n=4) and DEP-1 knockout mice (DEP-1 KO, n=4) were pre-injected intravenously with vehicle or 16 mg/kg AKB-9778 and after 30 minutes Evans blue dye was injected (1% in PBS, 100 µl) followed in 10 minutes by intradermal injections at three positions on the back with PBS, 100ng murine VEGF or 225ng histamine. After 30 minutes mice were euthanized, dye was extracted from skin, and quantified. The bars show mean (±SEM) fluorescence and statistical comparisons showed that in both WT and DEP-1 KO, AKB-9778 caused a significant reduction in VEGF-induced and histamine-induced dye leakage (*$p<0.01$ by ANOVA with Dunnett's correction for difference from VEGF/vehicle control;**$p<0.01$ for difference from histamine/vehicle control). (B) Lungs were dissected from four AKB-9778-treated mice (WT1, WT2, DEP-1 KO 1, and DEP-1 KO 2) and four vehicle-treated mice (WT3, WT4, DEP-1 KO 3, and DEP-1 KO 4) and lung lysates in RIPA buffer were analyzed. Immunopreciptation of Tie-2 followed by immunoblotting with antibodies against phosphotyrosines (4G10) and Tie-2 (3G1) showed that AKB-9778 increased Tie2 phosphorylation in both WT and DEP-1 KO mice. Immunoblotting of lung lysates for DEP-1 confirmed absence of DEP-1 in the DEP-1 KO mice. Molecular weight markers are indicated on the left.

Supplemental Figure 3

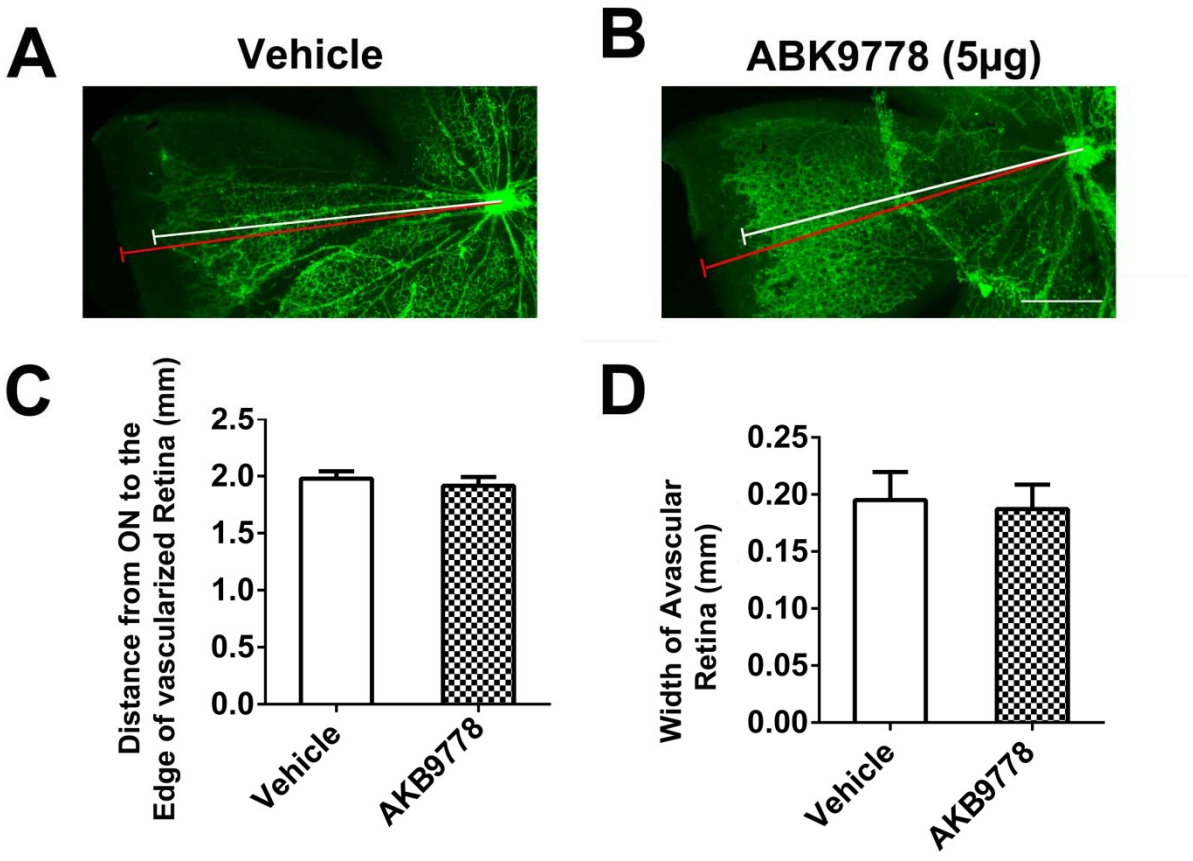

Supplemental Figure 3. Intraocular injection of AKB-9778 has no effect on vascularization of the surface of the retina.

C57BL6 mice (n=10) were given an intraocular injection of 5 µg of AKB-9778 or vehicle at P4. At P7 mice were euthanized and retinas were dissected, stained with FITC-GSA, and flat mounted. A masked observer measured the distance from the optic nerve (ON) to the peripheral edge of the developing retinal vasculature and the distance from the edge of the vasculature to the edge of the retina (width of avascular retina). Measurements were made in each of the 4 quadrants of the retina and the average was used as a single experimental value. The retinal vasculature appeared normal and similar in retinal flat mounts from vehicle-injected (A) and AKB-9778-injected eyes (B, bar=500µm). (C) The bars show the mean (±SEM) distance from optic nerve to vascular front and there was no significant difference in vehicle-injected versus AKB-9778-injected eyes. (D) The bars show the mean (±SEM) width of avascular retina and there was no significant difference in vehicle-injected versus AKB-9778-injected eyes.

Table 1

IC_{50} (nM) for AKB-9778 vs a panel of diverse phosphatase enzymes*

Receptor Tyrosine Phosphatases							Cytoplasmic tyrosine phosphatases		
VE-PTP	HPTPη	LAR	HPTPε	CD45	HPTPμ	HPTPγ	PTP1b	TCPTP	SHP-1/SHP-2
0.017	0.036	295	14609	3302	7812	0.100	780	2150	1665/9045

* IC_{50}s (nM) for a variety of additional phosphatases were 20000 to >100000: cyctoplasmic tyrosine phosphatases HCPTPA, PRL3; Dual specificity phosphatases MKP-1, VHR; Serine/threonine phosphatases ALP, PP1γ